E-Journal of Advanced Maintenance Vol.9-1 (2017) 15-25
Japan Society of Maintenology

Effect of Scaly Structure on the Measurement of Pipe Wall Thickness using EMAT

Hongjun SUN[1], Ryoichi URAYAMA[2], Tetsuya UCHIMOTO[2], Fumio KOJIMA[2], Toshiyuki TAKAGI[2,*], Hiroshi ABE[3], Kunihiro KOBAYASHI[4]

[1] *Graduate School of Engineering, Tohoku University, 2-1-1 Katahira, Aoba, Sendai, Miyagi 980-8577, Japan*
[2] *Institute of Fluid Science, Tohoku University, 2-1-1 Katahira, Aoba, Sendai, Miyagi 980-8577, Japan*
[3] *Graduate School of Engineering, Tohoku University, 6-6-01-2 Aoba, Aramaki, Aoba, Sendai, Miyagi 980-8579, Japan*
[4] *Tohoku Electric Power Co., Inc., 1-7-1 Honcho, Aoba, Sendai, Miyagi 980-8550, Japan*

ABSTRACT

To use an electromagnetic acoustic transducer (EMAT) to measure the thickness of a carbon steel pipe wall, the electromagnetic acoustic resonance (EMAR) and pulse-EMAR methods have been proposed previously. In this paper, the EMAR and pulse-EMAR methods are used to measure the wall thickness of the dorsum part of a bent carbon steel pipe that has experienced flow accelerated corrosion (FAC). The received signals are processed using superposition of n^{th} compression (SNC). The measurement results obtained with the EMAR and pulse-EMAR methods are compared with equivalent measurements of minimum thickness using a caliper gauge, and the RMSE discrepancies are 0.24 mm and 0.36 mm, respectively. The results show that these discrepancies can be attributed to the scaly structures created by FAC. Further investigation shows that even larger discrepancies exist between the pulse-EMAR measurements and the minimum-thickness caliper measurements, again mainly in the parts affected by FAC. Typical parts of the pipe wall are observed using a three dimensional confocal laser scanning microscope, which reveals differently shaped scaly structures in different parts of the specimen. The pulse-EMAR signals are simulated numerically. These results show that the pulse-EMAR method measures thickness accurately in the initial stages of FAC, but that discrepancies gradually increase. The pulse-EMAR results include all the surface conditions in the measurement region under the probe. According to the numerical analysis, combining the pulse-EMAR and SNC methods might lead to the thickness of only the pristine part of the measurement area being registered, which might explain the discrepancies obtained in the measurements.

KEYWORDS

Electromagnetic Acoustic Transducer, Electromagnetic Acoustic Resonance, Pulse-EMAR, Flow Accelerated Corrosion, scaly structure, Ultrasonic

ARTICLE INFORMATION

Article history:
Received 13 January 2017
Accepted 11 May 2017

1. Introduction

Carbon steel pipes are used extensively in nuclear power plants and fossil fuel power plants, etc [1, 2]. The pipe wall thinning due to the flow accelerated corrosion (FAC) is an important form of age-related degradation [2-7]. A characteristic of FAC is a scaly structure that is produced on the inner surface of the pipe [3–7]. Therefore, operational safety depends crucially on being able to measure the wall thickness accurately. At present, this is usually done by ultrasonic testing (UT) using an ultrasonic thickness gauge. However, such UT thickness measurements using the ultrasonic thickness gauge require some form of couplant liquid between the sample and the transducer. Not only is this very often practically inconvenient in the field, but also it makes it difficult to perform reproducible measurements [8]. In contrast, an electromagnetic acoustic transducer (EMAT) can generate elastic waves in an electrically conductive material without requiring any mechanical contact with the specimen [9, 10]. As such, EMAT has been applied in the field of non-destructive testing because of

*Corresponding author, E-mail: takagi@ifs.tohoku.ac.jp

its contactless characteristic. Therefore, it doesn't need couplant liquid and suits for measurement at high temperature.

The electromagnetic acoustic resonance (EMAR) method uses an EMAT to generate ultrasound in a specimen. If the total propagation distance is an integer multiple of the ultrasonic wavelength, the ultrasound is strengthened by resonance phenomena. The pulse-EMAR method uses an EMAT to generate a pulse wave in a specimen. The thickness of the specimen is obtained by analyzing the frequency components of the echo wave [11, 12].

The basic signal processing method for ultrasonic thickness measurement is the echo time method, which uses the time difference between the two echo signals form bottom surface to calculate the distance of ultrasonic wave propagation in the specimen. The thickness d of the specimen is equal to half the propagation distance, namely

$$d = \frac{vt}{2}, \tag{1}$$

where v is the wave velocity of ultrasound and t is the time difference of the two echoes signal.

Because the transduction efficiency of an EMAT is very low [8-10], a low signal to noise ratio is obtained when using the EMAR and pulse-EMAR methods [11]. To resolve this problem, Urayama et al. proposed processing the received signal using a method known as superposition of n^{th} compression (SNC) [11, 13], and they used the EMAR method combined with SNC signal processing to measure the thickness of pipes in a nuclear power plant. The SNC method superimposes the peak value of the frequency of each order of resonance on the peak value of the fundamental resonance frequency. It can be expressed as

$$f_1 = \arg\max_f \left\{ \sum_n x(nf) \right\}, \tag{2}$$

where f_1 is the fundamental resonance frequency, $x(f)$ is the SNC spectrum intensity, “arg max” is the frequency at which the SNC spectrum intensity is maximum, n is the superimposed resonance order. The peak value of the fundamental resonance frequency is SNC peak value. The SNC method has obtained good signal to noise ratio [11, 13]. Hence, according to the theory of ultrasonic resonance, the specimen thickness d can be calculated by

$$d = \frac{v}{2f_1}. \tag{3}$$

In previous studies, scaly structures as one of factors that may affect the measurement results were briefly discussed [13]. However, it only treated a special specimen to simulate artificial scaly structures. There has been no discussion about the scaly structures of an actual pipeline, and there was no numerical simulation of the effect of scaly structures. The purpose of this paper is to study the effect on EMAT measurements of pipe-wall thickness of the scaly structures that form on the inner surface of the pipe because of FAC. Therefore, in this study, the wall thickness of the dorsum part of a bent carbon steel pipe was measured using the EMAR and pulse-EMAR methods. As a comparison, measurements were performed in the same place using a caliper gauge. We then observed typical features of the scaly structure using a three-dimensional (3D) confocal laser scanning microscope (CLSM), as well as simulating the pulse-EMAR method numerically. All received signals were processed using the SNC method. Finally, the experimental and numerical results are discussed in relation to the scaly structures.

2. Experiments

2.1 Wall thickness measurement for an actual pipe

The specimen is the dorsum part of a bent carbon steel pipe from a fossil fuel power plant [3], and it is shown schematically in Fig. 1 (a). The dorsum part is cut into 12 parts. Part of the inner surface of the dorsum is covered in a scaly structure associated with FAC. The outer and inner diameters of the bent pipe are 139.8 mm and 126.6 mm, respectively. The nominal thickness of the bent pipe wall is 6.6 mm, and the radius of curvature of the bent pipe is 420 mm. The dorsum of the bent pipe has five measurement points in the circumferential direction and 23 measurement points in the pipe (i.e., flow) direction, as shown in Fig. 1(b).

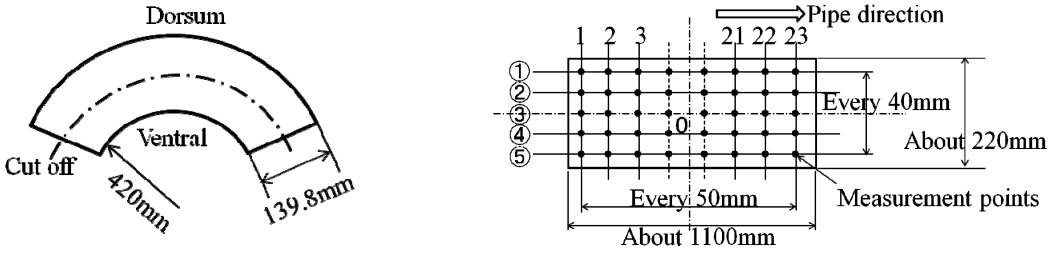

(a) Bent pipe shape (b) Measurement points of dorsum

Fig. 1. Specimen and measurement points

The diameter of the transmitter EMAT coil is 10 mm (40 turns) and the diameter of the receiver EMAT coil is 20 mm (80 turns). They are placed under a samarium–cobalt (SmCo) permanent magnet ($10 \times 20 \times 20\ mm^3$). Figure 2 shows the EMAT probe schematically. The complete thickness measurement system is shown in Fig. 3. In the EMAR method, the transmitter frequency range is 1–2.5 MHz. In the pulse-EMAR method, the center frequency of the pulse wave is 2 MHz. For comparison, the same measurements were performed using a caliper gauge with which the minimum thickness of the measurement point area could easily be measured [3]. As for the maximum thickness, we measured at numerous points close to the measurement point and took the maximum value as the maximum thickness of the measurement point area.

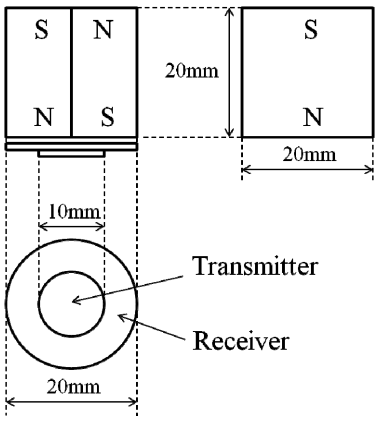

Fig. 2. EMAT probe

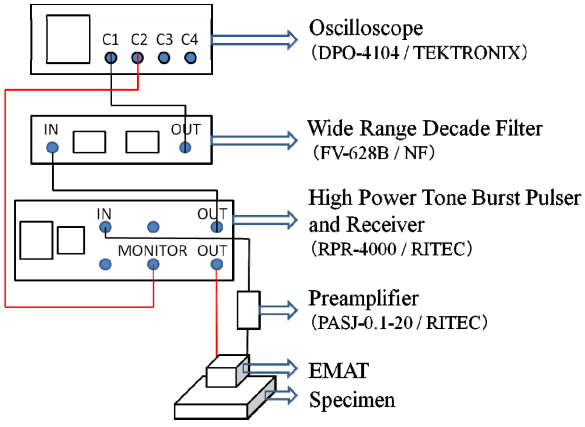

Fig. 3. System of EMAT thickness measurement

2.2 Thickness measurement results

The EMAR and pulse-EMAR received signals were processed using the SNC method, the analytical range of which is 1–3.5 MHz. Figure 4 shows separate comparisons of the EMAR and pulse-EMAR measurement results with the minimum measurement results made using the caliper gauge. These comparisons show that there was good agreement between the EMAR/pulse-EMAR and caliper measurements for some thicknesses but discrepancies for others. The largest of these discrepancies are 0.79±0.24 mm (EMAR) and 1.32±0.36 mm (pulse-EMAR), where each error is the

respective root-mean-square error (RMSE).

We select four specimens sequentially from the middle part of the pipe and refer to them as specimens A, B, C, and D. Specimen A is in the initial stages of FAC and has almost no scaly structure. Specimen B has a little wall thinning and a large number of scattered scaly structures. Specimen C has obvious wall thinning and is covered with large scaly structures. Specimen D has severe wall thinning and is covered with dense small scaly structures.

We select three representative measurement points on each specimen and number them as 1–3. The measurement results for all points are listed in Table 1. For specimens B and C, the measurement results made using the pulse-EMAR method are almost the same as the maximum thicknesses determined using the caliper gauge. For specimen D, the measurement results made using the pulse-EMAR method fall between the maximum and minimum thicknesses determined using the caliper gauge.

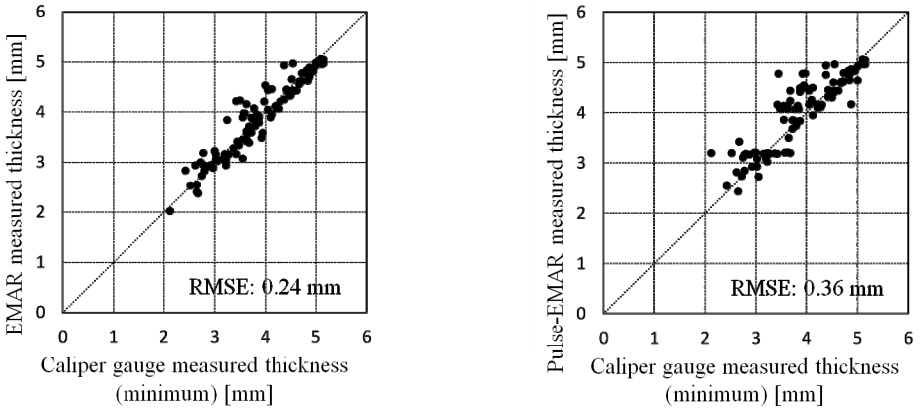

Fig. 4. Comparison of thickness measurement results

Table 1 Thickness measurement results for specimens A, B, C, and D (unit: mm)

Point	Pulse-EMAR	Caliper gauge (min)	Caliper gauge (max)
A-1	4.96	5.00	*
A-2	4.62	4.65	*
A-3	4.92	4.90	*
B-1	4.11	3.36	4.20
B-2	4.75	3.58	4.80
B-3	3.95	3.33	3.95
C-1	4.14	3.15	4.23
C-2	4.13	3.30	4.25
C-3	3.17	2.65	3.58
D-1	3.11	2.63	3.38
D-2	3.19	3.10	3.95
D-3	2.81	2.35	3.15

* There was no obvious concavity at the measurement points of specimen A. Therefore, the thickness at each of those three measurement points is listed as the minimum thickness only.

2.3 Discussion and micro-observation of the scaly structure parts

A transducer measures over an area of a specimen, not at a point. The measurement results correspond to the overall situation within this area. The reverberation surface of a part with a scaly structure is not smooth, such that the ultrasound experiences oblique incidence. This may lead to different mode conversion and energy partitioning for longitudinal and shear waves [14, 15], which in turn can lead to poor repeatability of the measurement results. Therefore, a scaly internal structure is often the main cause of discrepancies in the measurement results.

As can be seen in Fig. 4, the data points associated with the pulse-EMAR method are distributed mainly above and to the left of the isoline. This means that the thickness measured using the pulse-EMAR method tends to be larger than the minimum thickness measured using the caliper gauge. The largest such discrepancies are mainly in the thickness range of 3–5 mm by the pulse-EMAR method. From Table 1, the measurement results for specimen A are the most accurate, which is unsurprising because specimen A is similar to a flat plate. Specimens B and C have more scaly structures than flat parts. The pulse-EMAR measurement results for specimens B and C are closer to the maximum caliper thicknesses than to the minimum ones. This means that the reflected signal is dominated by the more coherent component from the flat parts. For specimen D, the pulse-EMAR measurement results fall between the minimum and maximum caliper thicknesses. Any part of a measurement area that is found to be pitted is deemed to be a scaly structure [3]. Synthesizing the above analyses, it is clear that the scaly area ratio has an appreciable influence on the measurement of thickness.

The actual surface topographies in the scaly parts of specimens A, B, C, and D were observed using a 3D CLSM (VK-X 100; Keyence Corp.). Surface modification was used to process the original results because the specimens were from a bent pipe. A single scan took about 1 h. Figure 5 shows 3D images of the measured areas, the dimensions of which are 11,240.6 μm × 800.0 μm (points A-1, B-1, and C-1) and 8,780.5 μm × 7,199.5 μm (point D-1). For comparison, the surface profile of the middle section of each specimen is shown in Fig. 6. The ordinate is the depth from the highest point of the measurement area. In the measurement areas of specimens A, B, C, and D, the scaly area ratios are 0, 71.2%, 88.2%, and 100%, respectively. The maximum depths of the surface pits are 0, 1,090 μm, 1,416 μm, and 1,176 μm, respectively. In the measurement area of point D-1, small dense scaly structures due to a large number of large block scaly pits mutual interference. The maximum depth of the pits in the region in which mutual interference occurs is 774 μm. Based on the above observations, we now proceed to numerical simulations of the effect of various scaly area ratios on the EMAT thickness measurements.

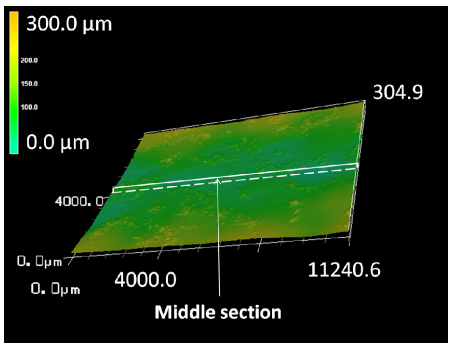

Point A - 1

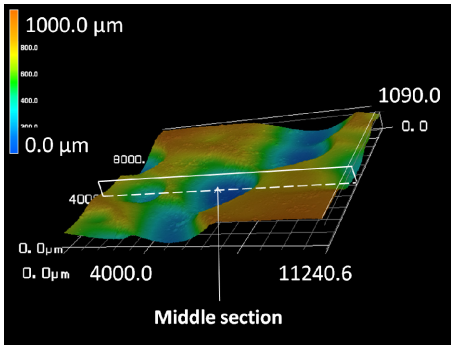

Point B – 1

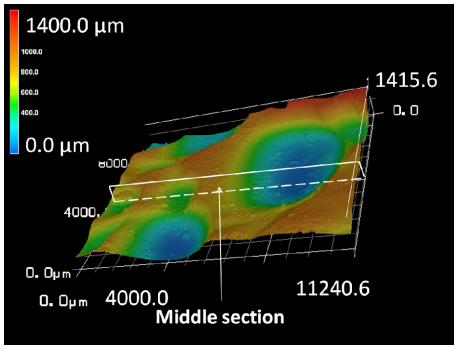

Point C - 1

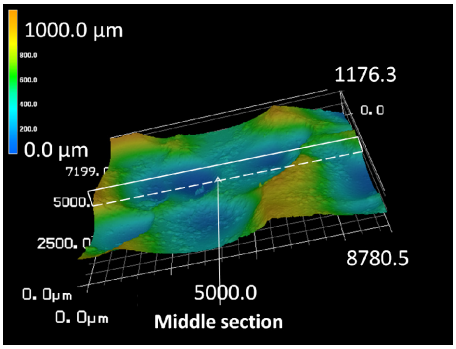

Point D – 1

Fig. 5. 3D images of measured areas

3. Numerical simulations of Pulse-EMAR

In order to confirm that the EMAR and pulse-EMAR methods give larger thickness values compared to the caliper gauge results, we performed numerical simulations. To evaluate the pulse-EMAR method of measuring the wall thickness of a carbon-steel pipe, we developed a 3D finite element (FE) model, the geometry of which is shown in Fig. 7. The FE model consists of two simulation parts: the electromagnetic field and the ultrasonic propagation. These are simulated using the commercial software GiD and ComWAVE (Itochu Techno-Solutions Corp.), respectively, with the two parts coupled via the electromagnetic force.

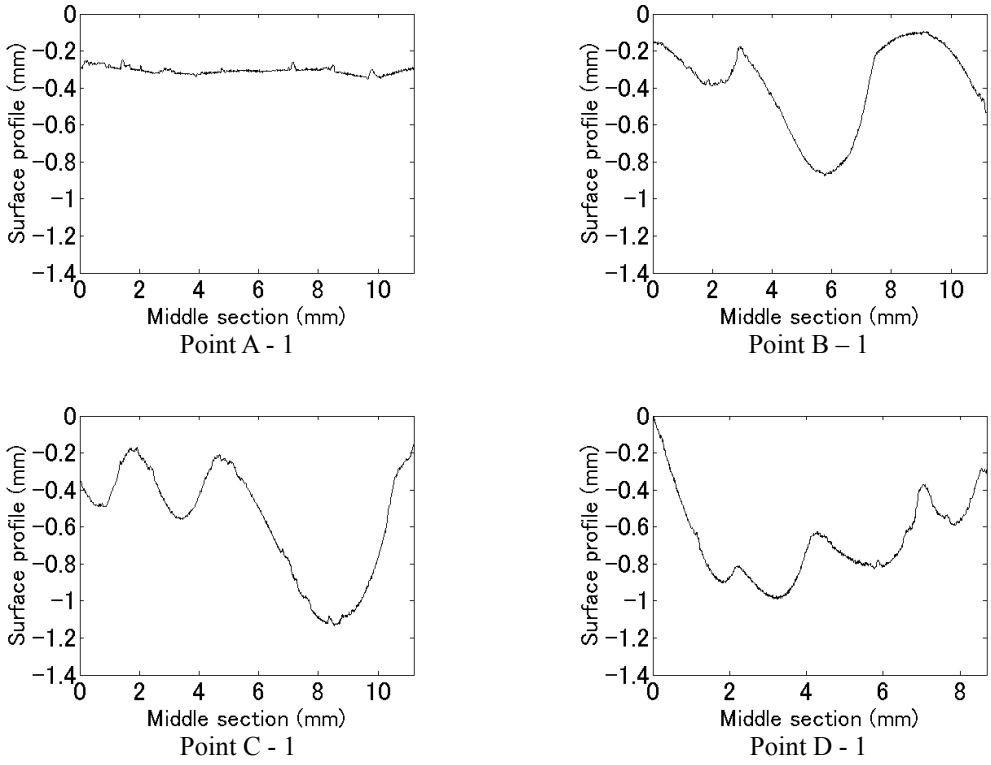

Fig. 6. Surface profiles of middle sections in Fig. 5

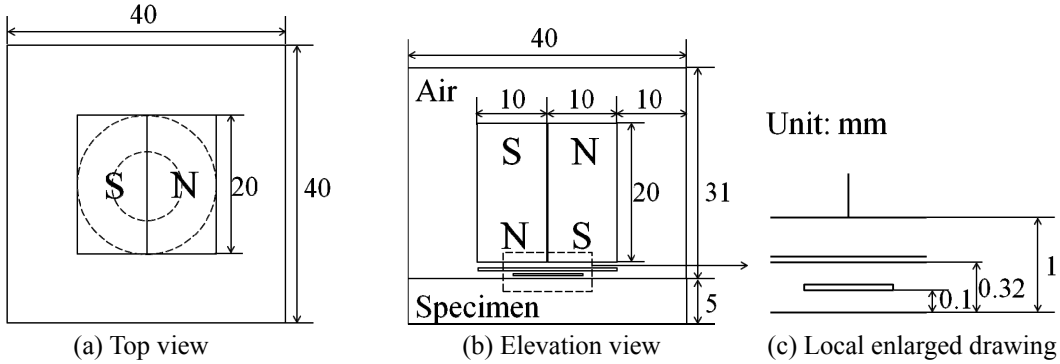

Fig. 7. Geometries of finite element (FE) model

3.1 Coupling of electromagnetic and mechanical mechanisms

In ferromagnetic materials, the transformation mechanism between electromagnetic field and elastic wave includes Lorentz force, magnetization force and magnetostrictive force. They can be expressed as [8],

$$\boldsymbol{F}^{L} = \boldsymbol{J} \times \boldsymbol{B}, \tag{4}$$

$$\boldsymbol{F}^{M} = (\nabla \boldsymbol{H}) \cdot \boldsymbol{M}, \tag{5}$$

$$\boldsymbol{F}^{MS} = \nabla \cdot (\boldsymbol{e} \cdot \boldsymbol{H}), \tag{6}$$

where $\boldsymbol{F}^{L}$ is the Lorentz force, $\boldsymbol{J}$ is the eddy current, $\boldsymbol{B}$ is the magnetic flux density, $\boldsymbol{F}^{M}$ is the magnetization force, $\boldsymbol{H}$ is the magnetizing field, $\boldsymbol{M}$ is the magnetization, $\boldsymbol{F}^{MS}$ is the magnetostrictive force, and $\boldsymbol{e}$ is the tensor of the magnetostriction.

The magnetization force is very weak, and hence we choose to ignore it. In this study, the magnetostrictive force is also neglected because the Lorentz force is the dominant transduction mechanism in a strong static magnetic field [8, 9].

3.2 Electromagnetic field simulation implementation

The electromagnetic model was implemented using the software GiD by discretizing the domain into 136,800 hexahedron elements as shown in Fig. 8 (elevation view). The strength of the field generated with the permanent (SmCo) magnet employed is 1 T. The coil carries a 10 A current that oscillates at a frequency of 2 MHz. The specimen material is low carbon steel with an electrical conductivity of 5.26×10^{6} S/m and a relative permeability of 100 [16]. The FE mesh is refined near the specimen surface because of the skin effect of the eddy current.

The distribution of the Lorentz force is calculated using the Lorentz-force calculation module because of the distributions of the static magnetic field and the eddy current. The Lorentz force is used subsequently to generate ultrasound in the ultrasonic propagation simulation. The calculation time of the FE model was approximately 20 min (Intel Core i7 4790, 3.6 GHz, 8 GB).

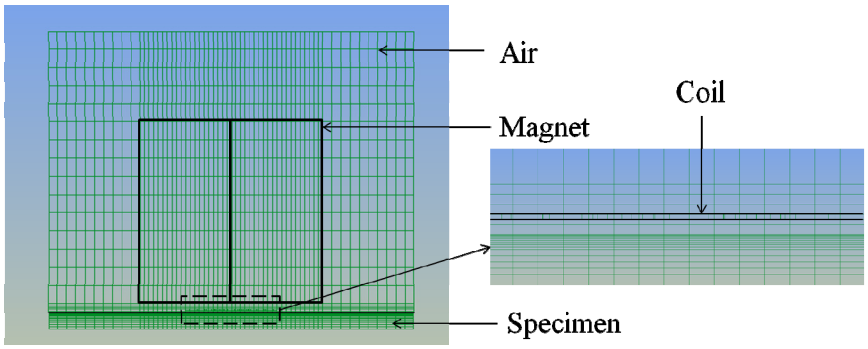

Fig. 8. Meshes of FE model

3.3 Ultrasonic propagation simulation implementation

The ultrasonic propagation model was set up using the software ComWAVE. To simulate the pits of the scaly structures due to FAC, the lower surface of the specimen was indented with partial spheres. In this study, according to the measurement results in Sect. 2.3, the four specimens shown in Fig. 9 were calculated. Model I simulates specimen A, which has a smooth reflection surface. Model II simulates specimen B, by indenting the lower surface with partial spheres of diameter 4.74 mm and height (depth) 1.10 mm. In order to realize a scaly area ratio of about 71.2%, we set the gap between adjacent rows of partial spheres to 0.5 mm; this gave a scaly area ratio of 69.8% and a thickness range in the pitted regions of 3.90–5.00 mm. Model III simulates specimen C and is similar to model II. However, the diameter and depth of the partially spherical indentations are now 7.82 mm and 1.40 mm, respectively. The intentions are also now more closely arranged such that the scaly area ratio is 90.7%, and the thickness range in the pitted regions is 3.60–5.00 mm. Model IV simulates specimen D and is similar to models II and III. However, the diameter and depth of the partially spherical indentations are now 9.20 mm and 1.20 mm, respectively. There is also overlap between neighboring indentations, and the thickness range in the pitted regions is 3.80–4.60 mm. All the simulation parameters are listed in Table 2.

Each of the four models is divided into a different number of hexahedron elements: 4,300,800

(model I), 4,161,512 (model II), 4,055,504 (model III), and 4,045,628 (model IV). In order to reduce the effect of reflection, absorption bands (3 mm thick) are set on the side surfaces of the specimens. The density of the material is 7,850 kg/m^3. The shear wave and longitudinal wave velocities are 3,230 m/s and 5,950 m/s, respectively. Near the specimen upper surface, the meshes are refined because of the skin effect of the eddy current. The ultrasonic propagation process is calculated over the first 1.1×10^{-4} s. The calculation time of the FE model is about 46 h (Intel Core i7 4790, 3.6 GHz, 8 GB).

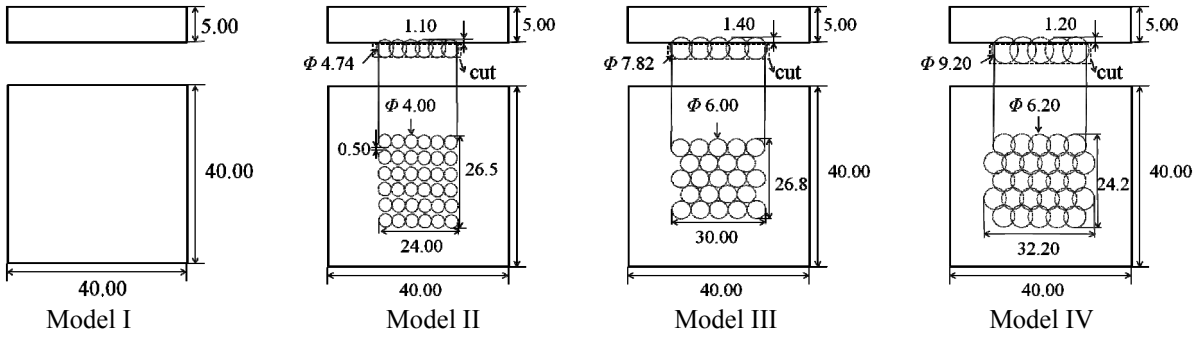

Fig. 9. Specimen models (unit: mm)

Table 2 Simulation parameters of the specimen models

	Scaly area ratio	Thickness of scaly area	Maximum depths of the pits	Depth of mutual interference parts
Model I	0	5.00 mm	0	-
Model II	69.8%	3.90–5.00 mm	1.10 mm	-
Model III	90.7%	3.60–5.00 mm	1.40 mm	-
Model IV	100%	3.80–4.60 mm	1.20 mm	0.80 mm

3.4 Results and discussion

In order to compare with experiments, the analytical range of the SNC method was set to 1000–3500 kHz. Figure 10 shows the FFT spectrum on the analytical range over the SNC for the four models. All data have been normalized on the maximum SNC value of the specimen without scaly structure (model I). Figure 11 shows the SNC spectrum for the four models. For comparative purposes, we set the peak value for model I to unity and normalize the other data accordingly. All the results are listed in Table 3. The thickness values of models I–IV obtained by the SNC method are almost within the true thickness range, which demonstrates the validity of the SNC method. When the reflection surface is uneven, such as for models II–IV, the SNC peak values decrease rapidly. The thicknesses of models II and III obtained by the SNC method are close to the maximum thickness. This is because 30.2% and 9.3%, respectively, of the measurement area is not scaly. For model IV, the thickness obtained by the SNC method is between the minimum and maximum thicknesses. These results are in agreement with the experimental results. Therefore, the proportion of the measurement area that is scaly may affect the measurement results.

The effects of a scaly structure on the measurement of pipe wall thickness can be divided roughly into four cases: specimens A–D or models I–IV. In model I, the SNC-calculated thickness accurately reflects the actual thickness of the pipe wall. In models II and III, the SNC-calculated thickness is approximately that of the flat part (i.e., the maximum thickness). In this case, the result of the pulse-EMAR method is larger than the minimum thickness. In model IV, although the wall thinning is more serious, the measurement results are close to the minimum wall thickness. There are some discrepancies in the EMAR and pulse-EMAR measurement results and the minimum thicknesses obtained with the caliper gauge. This is essentially because the EMAR and pulse-EMAR methods measure over an area, not at a point. Hence, the EMAR and pulse-EMAR results include surface

information from the whole measurement region under the probe. According to the numerical results, the spectrum includes several peaks, which might reflect the surface conditions. However, the SNC result might give the thickness of the flat surface. The Pulse-EMAR method gives accurate thickness measurement results. From the numerical results, we see for models II and III that the method might give the maximum thickness. This might explain the discrepancies obtained in the measurements. In order to obtain better results, the thickness of a smaller measurement area could be assessed by reducing the transducer size or focusing the ultrasound, hence better approximating the conditions at the actual measurement point. Therefore, in future work, we intend to improve the design of the transducer so that it generates and receives stronger ultrasonic signals over a smaller area.

4. Conclusions

In this study, the wall thickness of the dorsum part of a corroded bent carbon steel pipe was measured using the EMAR and pulse-EMAR methods and with a caliper gauge, and the results were compared. The caliper/EMAR and caliper/pulse-EMAR RMSE discrepancies were 0.24 mm and 0.36 mm, respectively. The results show that the scaly structure owing to FAC leads to discrepancies between the various measurement results. To reveal the effects of this scaly structure on the measurement of pipe wall thickness, typical parts of the pipe wall were observed using 3D CLSM. This led on to numerical simulations of the effects of various scaly structures on the pulse-EMAR thickness measurements. The received signal was processed using the SNC method, which showed that the proportion of scaly structure in the measurement area can affect the measurement results. This agrees with the results of the experiments mentioned above.

Overall, the results show that the pulse-EMAR method measures thickness accurately in the initial stage of FAC, after which the discrepancies gradually increase. It is even possible for the pulse-EMAR method to return the thickness of the flat regions in the measurement area under the probe, which might explain the discrepancies obtained in the measurements.

Shrinking the transducer or focusing its waves would allow thickness to be measured over a smaller area. This would bring the measurement results closer to the actual thickness at the measurement point.

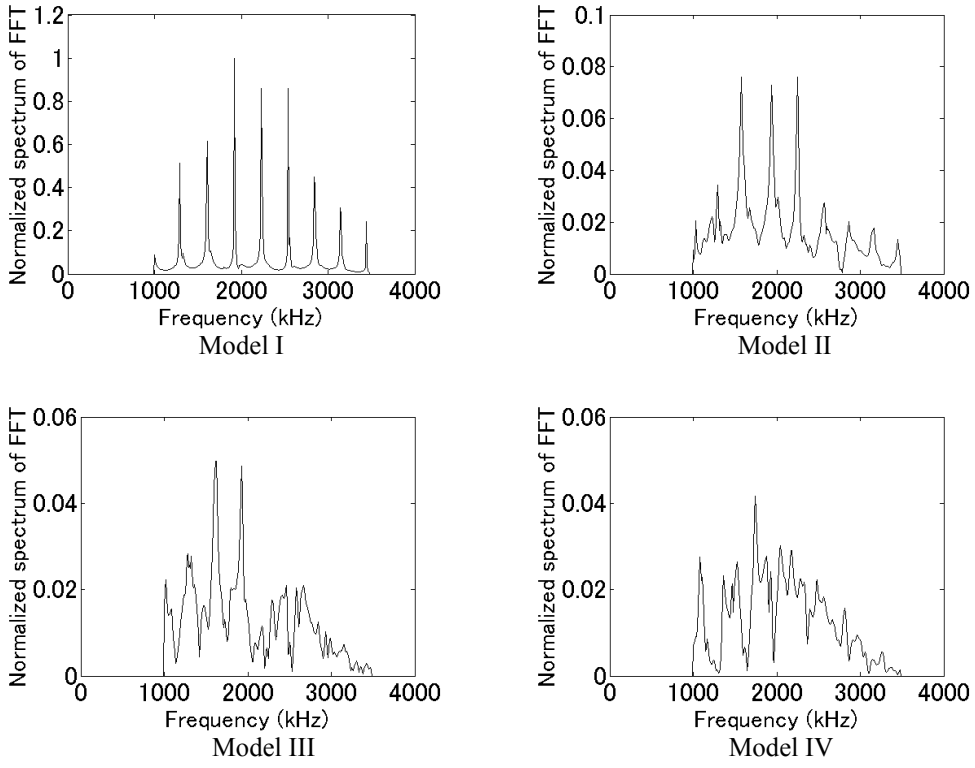

Fig. 10. FFT spectrum of specimens

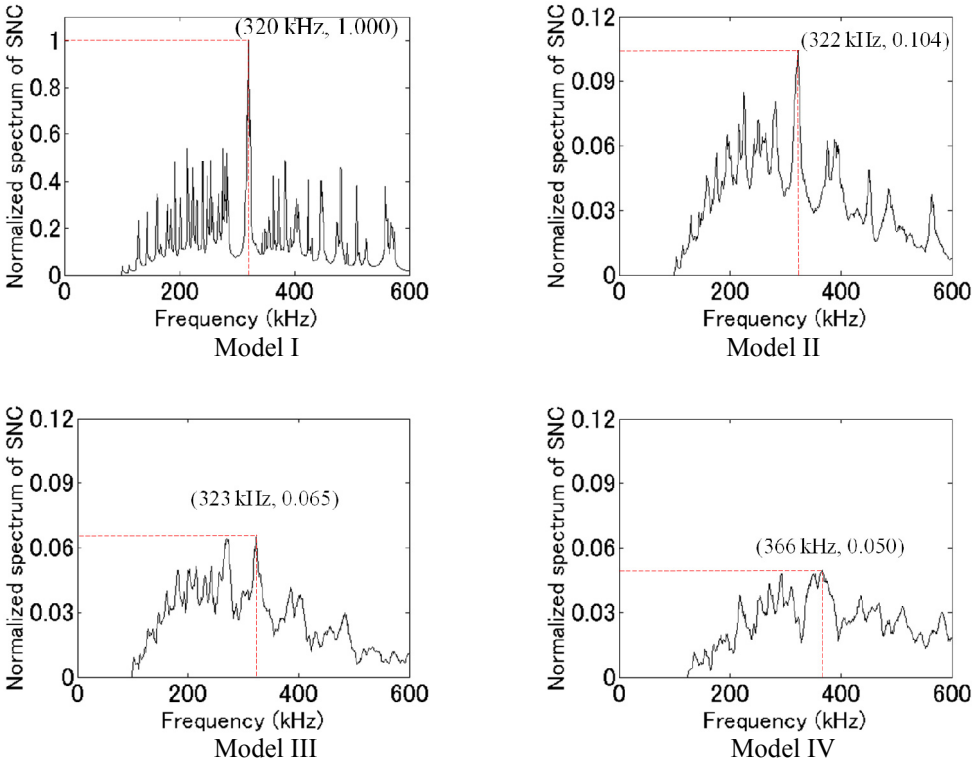

Fig. 11. SNC spectrum of specimens (analytical range of SNC method: 1000 – 3500 kHz)

Table 3 simulation results (analytical range of SNC method: 1000 – 3500 kHz)

	Real thickness of scaly structure area	Fundamental resonant frequency of SNC	Thickness by SNC method	Normalized SNC peak value
Model I	5.00 mm	320 kHz	5.05 mm	1.000
Model II	3.90 - 5.00 mm	322 kHz	5.02 mm	0.104
Model III	3.60 - 5.00 mm	323 kHz	5.00 mm	0.065
Model IV	3.80 - 4.60 mm	366 kHz	4.41 mm	0.050

Acknowledgements

This work was partly supported by 1) the JSPS Core-to-Core Program, A. Advanced Research Networks, “International research core on smart layered materials and structures for energy saving”, 2) the “Fundamental Research and Human Resources Development Program for Nuclear Decommissioning related to Integrity Management of Critical Structures including Primary Containment Vessel and Reactor Building, and Fuel Debris Processing and Radioactive Waste Disposal” by the Ministry of Education, Culture, Sports, Science and Technology of Japan, and 3) by an IFS Research Assistant Award for International Students. The authors are grateful to the Hashizume Laboratory of Tohoku University for offering the use of the 3D CLSM.

References

[1] F. Masuyama: "History of power plants and progress in heat resistant steels", ISIJ International, Vol. 46, pp. 612-625 (2001).
[2] W. H. Ahmed: "Flow accelerated corrosion in nuclear power plants", INTECH Open Access Publisher, 2012.
[3] H. Abe, Y. Watanabe, M. Nakashima, T. Tatsuki: "Characterization of corroded surface morphology of

carbon steel piping elbow affected by Flow-Accelerated Corrosion", E-Journal of Advanced Maintenance, 2017.

[4] H. Abe, T. Yano, Y. Watanabe, M. Nakashima, T. Tatsuki: "Characteristics of scalloped surface and its relation to FAC rate of carbon steel piping elbow", Transactions of the JSME (in Japanese), 2017

[5] V. Kain, S. Roychowdhury, T. Mathew, A. Bhandakkar: "Flow accelerated corrosion and its control measures for the secondary circuit pipelines in Indian nuclear power plants", Journal of Nuclear Materials, Vol. 383, pp. 86-91 (2008).

[6] J. L. Singh, U. Kumar, N. Kumawat, S. Kumar, V. Kain, S. Anantharaman, A.K. Sinha: "Flow accelerated corrosion of carbon steel feeder pipes from pressurized heavy water reactors", Journal of Nuclear Materials, Vol. 429, pp. 226-232 (2012).

[7] V. Kain: "Flow accelerated corrosion: forms, mechanisms and case studies", Procedia Engineering, Vol. 86, pp. 576-588 (2014).

[8] R. Ribichini, P. B. Nagy, H. Ogi: "The impact of magnetostriction on the transduction of normal bias field EMATs", NDT and E International, Vol. 51, pp. 8-15 (2012).

[9] R. B. Thompson: "Physical principles of measurements with EMAT transducers", Physical Acoustics, Vol. 19, pp.157-200 (1990).

[10] H. Ogi, E. Goda, M. Hirao: "Increase of efficiency of magnetostriction SH-wave electromagnetic acoustic transducer by angled bias field: Piezomagnetic theory and measurement", Japanese Journal of Applied Physics, Vol. 42, pp. 3020-3024 (2003).

[11] R. Urayama, T. Takagi, T. Uchimoto, S. Kanemoto: "Online monitoring of pipe wall thinning by electromagnetic acoustic resonance method", E-Journal of Advanced Maintenance, Vol. 5, pp. 155-164 (2013).

[12] K. Kawashima, O. B. Wright: "Resonant electromagnetic excitation and detection of ultrasonic waves in thin sheets", Journal of Applied Physics, Vol. 72, pp. 4830-4839 (1992).

[13] R. Urayama, T. Takagi, T. Uchimoto, S. Kanemoto, T. Ohira, T. Kikuchi: "Implementation of electromagnetic acoustic resonance in pipe inspection", E-Journal of Advanced Maintenance, Vol. 5, pp. 25-33(2013).

[14] J. L. Rose: "Ultrasonic waves in solid media", Cambridge university press, 2004.

[15] L. W. Schmerr Jr: "Fundamentals of Ultrasonic Nondestructive Evaluation: A Modeling Approach", Springer Science and Business, 2013.

[16] Y. Katayama, M. Sakane, M. Ohnami: "Surface crack detection by A. C. Potential Drop method: Experiment and FEM considerations", Transactions of the Japan Society of Mechanical Engineers, Series A, Vol. 62, pp. 2216-2223 (1996).